MECSOL 2019 - Proceedings of the 7th International Symposium on Solid Mechanics
V. Tita, A. Ferreira, M.L. Ribeiro, A. Vieira and A.T. Beck (Editors), ABCM, Sao Carlos, SP, Brazil, April 15th to 17th, 2019

Topology optimization applied to the design of pneumatic actuators

Eduardo Moscatelli de Souza[1], Emílio Carlos Nelli Silva[1]

[1] Polytechnic School of the University of São Paulo, Av. Prof. Luciano Gualberto, 380 - Butantã, São Paulo - SP, 05508-010

Abstract. This work aims to apply the density-based topology optimization method to the design of pneumatic soft actuators. The approach employed involves the use of compliant mechanism formulations with pressure loading at input ports. The physical model used to represent the pressure loading is based on mixed finite elements. Besides our aim is to design pneumatic actuators, the same design was optimized for different fluids (air, water, and highly incompressible fluid) to evaluate the influence of the material properties in the optimization. We optimized a bending and a linear actuator considering solid isotropic linearly elastic material model and small displacement for the kinematic description. In both cases the convergence was easier for more incompressible fluids.
Keywords: soft actuators, topology optimization, mixed displacement-pressure

INTRODUCTION

The advances in software and electronics technologies and its applications to machine design has consolidated the use of robotics in industry. In last years it was also possible to see the expansion of robots to other fields closer to our daily life. However, certain limitations presented by components used in traditional robots, like poor performance in unstructured environments and difficulties dealing with fragile objects, motivated researchers to investigate the use of soft materials in the design of robots, actuators, and sensors, as can be seen in works such as Suzumori (1996), Galloway et al. (2013), and Mosadegh et al. (2014).

These soft components are designed for specific applications, so there is interest in automating the design procedure and techniques such as topology optimization presents great potential to the field. Some works, like Hiller and Lipson (2012), started investigating design automation employing topology optimization with evolutionary algorithms.

Topology optimization is a design method that aims to find the material layout that extremizes an objective function. The technique, introduced by Bendsøe and Kikuchi (1988), was created in the context of structural optimization, but it has already been applied to the design of compliant mechanisms (Pedersen, Buhl and Sigmund, 2001), minimization of energy dissipation in Stokes flow (Borrvall and Petersson, 2002), heat conduction problems (Gersborg-Hansen, Bendsøe, and Sigmund, 2006), and others engineering problems. It also received development to assert design constraints such as length (Guest, Prévost and Belytschko, 2004) and stress control (París et at, 2008).

Researchers have also developed different approaches for topology optimization in an attempt to overcome limitations of particular formulations. The main approaches are density methods (Bendsøe, 1989), level set methods (Allaire, Jouve, and Toader, 2002), phase field methods (Bourdin and Chambolle, 2003), and topological derivatives methods (Sokolowski and Zochowski, 1999).

This work studies the application of the density-based topology optimization method to the design of pressure driven soft actuators. The approach employed is based on the use of a mixed displacement-pressure formulation (Clausen and Sigmund, 2007) to the design of a compliant mechanism. We study the optimization of the interior surfaces of the actuator. Although our aim is to design soft actuators, this study considers linear models for the kinematics and the constitutive models to concentrate our effort on the topology optimization aspects of the design. Some material behaviors presented by rubbers (like stress softening) will not be addressed because they are not modelled by linear models.

FORMULATION

Topology Optimization

The topology optimization problem to be solved is to design a compliant mechanism driven by a pressure loading. According to Pedersen, Buhl and Sigmund (2001), the design of a compliant mechanism can be made by the maximization of the output displacement which is equivalent to the maximization of the output work. In this paper, we solved the optimization problem given by Eq. (1), in which the vector $\boldsymbol{l}$ gives the desired output direction, the vector $\boldsymbol{v}$ contains the volume of each finite element, and the system of equations $\boldsymbol{F}(\boldsymbol{u},\boldsymbol{\rho}) = \boldsymbol{0}$ represents the constraints that impose the physical model to the optimization process.

$$\begin{aligned} \max_{\boldsymbol{\rho}} \quad & J(\boldsymbol{u},\boldsymbol{\rho}) = \boldsymbol{l}^T \boldsymbol{u} \\ \text{s.t.} \quad & \boldsymbol{F}(\boldsymbol{u},\boldsymbol{\rho}) = \boldsymbol{0} \\ & V^* - \boldsymbol{v}^T \boldsymbol{\rho} \geq 0 \\ & \boldsymbol{0} \leq \boldsymbol{\rho} \leq \boldsymbol{1} \end{aligned} \tag{1}$$

The workpiece is modeled as a stiffness k_{out} and its contribution to the finite element model is given by the bilinear form of Eq. (2). The input port has no stiffness because we used pressure as actuating load.

$$A_{el}(\boldsymbol{u},\boldsymbol{\delta u}) = \int_{\Gamma_{out}} k_{out}(\boldsymbol{\delta u}\cdot\boldsymbol{l})(\boldsymbol{u}\cdot\boldsymbol{l})\, d\Gamma \tag{2}$$

Density filtering

The use of density filtering techniques in topology optimization ensures well-posed and mesh independent solutions. The disadvantage of density filtering is the introduction of grey transition regions between void and solid phase. In this work, we used the filtering technique proposed by Lazarov and Sigmund (2010) which is based on the solution of the Helmholtz equation presented in Eq. (3). In this equation, ρ is the design variable field, $\widetilde{\rho}$ is the filtered field, and w is a test function.

$$r^2 \int_\Omega \nabla\widetilde{\rho}\cdot\nabla w\, d\Omega + \int_\Omega \widetilde{\rho} w\, d\Omega = \int_\Omega \rho w\, d\Omega \tag{3}$$

Threshold projection

The threshold projection presented by Eq. (4) is used to remove intermediate densities induced by the density filtering. It was introduced in this format by Wang, Lazarov, and Sigmund (2010). This equation projects values above the threshold η to 1 and values below to 0. The parameter β controls the steepness of the transition from void to solid enabling the application of a continuation method that avoids local minimum points.

As pointed out by Wang, Lazarov, and Sigmund (2010), the use of threshold values $\eta \in]0,1[$ does not assert length scale on void or solid phases. However, the use of η close to 0.5 provides good convergence, so we choose $\eta = 0.5$ in our optimization routines.

$$\widehat{\rho}(\widetilde{\rho}) = \frac{\tanh(\beta\eta) + \tanh(\beta(\widetilde{\rho}-\eta))}{\tanh(\beta\eta) + \tanh(\beta(1-\eta))} \tag{4}$$

Physical Model

The design of pressure loaded devices by topology optimization method requires physical models that are able to represent the loaded surface throughout the optimization process. The model used in this work is a mixed displacement-pressure formulation proposed by Clausen and Sigmund (2007). It is able to model contained fluids by the use of conveniently chosen material constants.

Mixed displacement-pressure formulation

The equilibrium equation for a continuum Ω in weak form is given by Eq. (5), in which $\Gamma = \partial\Omega$ is the boundary surface of Ω, $\boldsymbol{\delta u}$ is a test function for the displacement field, $\boldsymbol{\varepsilon}$ is the strain tensor, $\boldsymbol{\sigma}$ is the stress tensor, $\boldsymbol{b}$ is the body forces field, and $\boldsymbol{t}$ is the traction forces field.

$$\int_\Omega \boldsymbol{\varepsilon}(\boldsymbol{\delta u}) : \boldsymbol{\sigma}(\boldsymbol{u})\, d\Omega = \int_\Omega \boldsymbol{\delta u}\cdot\boldsymbol{b}\, d\Omega + \int_\Gamma \boldsymbol{\delta u}\cdot\boldsymbol{t}\, d\Gamma \tag{5}$$

Considering a solid under small deformations, the strain tensor is given by the function $\boldsymbol{\varepsilon}(\boldsymbol{u}) = \frac{1}{2}\left(\boldsymbol{\nabla u} + \boldsymbol{\nabla u^T}\right)$. The test function $\boldsymbol{\delta u}$ must be chosen from a set of functions that satisfy the Dirichlet boundary conditions.

By considering the isotropic linearly elastic material model, two materials constants are required to represent the material behavior. The two most common parameters are the Young's modulus (E_Y) and the Poisson's ratio (ν) due to its physical interpretation. Other common parameters are the Lamé's parameters λ and μ that are widely used to write the mathematical description of an isotropic linearly elastic material given by Eq. (6).

$$\boldsymbol{\sigma}(\boldsymbol{u}) = 2\mu\boldsymbol{\varepsilon}(\boldsymbol{u}) + \lambda \mathrm{tr}(\boldsymbol{\varepsilon}(\boldsymbol{u}))\boldsymbol{I} \tag{6}$$

In Clausen and Sigmund (2007), the authors used the bulk modulus (K) and the shear modulus (G). The shear modulus is exactly the second Lamé's parameter (μ). The bulk modulus is defined as the relation between the applied pressure on a material particle and its volumetric strain (dilatation). For small deformations, the dilatation is defined by Eq. (7).

$$\boldsymbol{e}(\boldsymbol{u}) = \mathrm{tr}(\boldsymbol{\varepsilon}(\boldsymbol{u})) = \nabla \cdot \boldsymbol{u} \tag{7}$$

So, the bulk modulus relates pressure and displacement according to Eq. (8). This equation and the result of its substitution on the later equations form the mixed problem to be solved.

$$p = -K\nabla \cdot \boldsymbol{u} \tag{8}$$

In weak form, the equilibrium is written by the system of equations formed by Eqs. (9) and (10), where $\boldsymbol{\varepsilon}'$ is the deviatoric strain tensor.

$$\int_\Omega \boldsymbol{\varepsilon}(\boldsymbol{\delta u}) : 2G\boldsymbol{\varepsilon}'(\boldsymbol{u})\, d\Omega - \int_\Omega \boldsymbol{\varepsilon}(\boldsymbol{\delta u}) : p\boldsymbol{I}\, d\Omega = \int_\Omega \boldsymbol{\delta u}\cdot\boldsymbol{b}\, d\Omega + \int_\Gamma \boldsymbol{\delta u}\cdot\boldsymbol{t}\, d\Gamma \tag{9}$$

$$\int_\Omega \delta p\,(p/K + tr(\boldsymbol{\varepsilon}))\, d\Omega = 0 \tag{10}$$

The deviatoric strain tensor is the result of the subtraction of the hydrostatic component of the strain tensor from itself according to Eqs. (11) and (12).

$$\boldsymbol{\varepsilon}'(\boldsymbol{u}) = \boldsymbol{\varepsilon}(\boldsymbol{u}) - \frac{1}{3}\mathrm{tr}(\boldsymbol{\varepsilon}(\boldsymbol{u}))\boldsymbol{I} \qquad \text{for 3D} \tag{11}$$

$$\boldsymbol{\varepsilon}'(\boldsymbol{u}) = \boldsymbol{\varepsilon}(\boldsymbol{u}) - \frac{1}{2}\mathrm{tr}(\boldsymbol{\varepsilon}(\boldsymbol{u}))\boldsymbol{I} \qquad \text{for 2D} \tag{12}$$

RESULTS

The numerical simulations were performed using the FEniCS computing platform (Alnaes et al, 2015; Logg et al, 2012) for the finite element analysis, Ipopt package for large scale nonlinear optimization (Wächter and Biegler, 2006), and dolfin-adjoint for the sensitivity analysis (Farrell et al, 2013; Funke and Farrell, 2013). This section starts with the evaluation of the developed code to reproduce results found in literature. Than, it presents the results obtained with the proposed formulations.

Verification of optimization routines

We evaluated the ability of our optimization routines to reproduce literature results with the bridge example presented in Clausen and Sigmund (2007). Figure 1 shows the design domain (Fig. 1a) for the problem and the results obtained with a classical pure displacement (Fig. 1b) approach and with the mixed approach (Fig. 1c). The differences between our results and the ones presented in the cited paper are due to the filter used.

Soft Actuators

The problem considered to evaluate the ability of the presented formulations to design pneumatic and hydraulic actuators is to maximize the output port displacement of actuators pressurized at its input port. Two designs were considered: a bending and a linear actuator.

(a) Design domain (b) Standard displacement topology (c) Mixed formulation topology

Figure 1: Results for bridge example considering standard displacement and mixed formulation. Figure 1a was extracted from Clausen and Sigmund (2007)

It is important to have in mind during the analysis of the results that the internal shape of the actuator does not change the resultant load over its surface. It changes only the local stiffness of the surface increasing or decreasing its displacement. As a consequence we expect to find wall modifications (Fig. 2a) and we do not expect internal complex structures (Fig. 2b) that have low impact on wall stiffness.

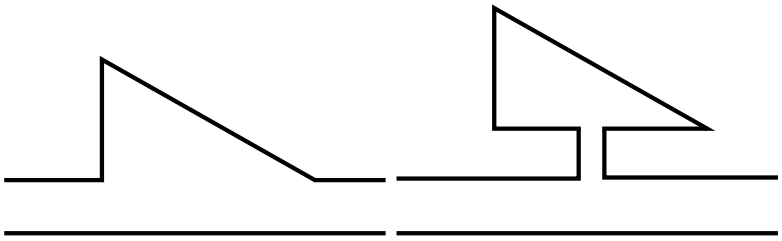

(a) Expected topology (b) Not expected topology

Figure 2: Examples of wall topologies. Figure 2a is an expected topology because it changes the stiffness of the wall. Figure 2b is not expected because it has low impact on wall stiffness.

Bending soft actuator

The most commom soft actuators found in literature are the ones with bending capabilities. To design this kind of actuator we used a rectangle domain of dimensions L and H. The input port is centered at left edge and it is limited by two support regions of length t. The output port is localized at the right lower corner of the design domain. Figure 3 illustrates this problem.

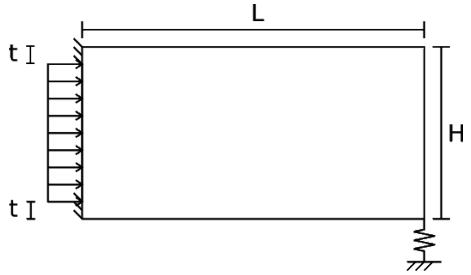

Figure 3: Design domain for the bending soft actuator.

For the bending actuator optimization we considered a geometry of $L = 20$ m, $H = 10$ m, $t = 1$ m. The solid material properties were based on high carbon steel: $E = 210$ GPa, and $\nu = 0.3$. Besides soft actuators are not fabricated from steel, this simplification was made as a first study of the presented formulations in the design of soft actuators. The volume constraint was set to half of the design domain ($V^* = 0.5 \cdot L \cdot H$).

The finite element discretization was made with right triangular elements. We used quadratic shape functions for displacement interpolations and linear shape functions for pressure and design variables. The linear interpolation for

design variables is required to solve the Helmholtz equation. The density filter length parameter was chosen to be r = 1 m while the element size chosen was 0.25 m. The continuation of the threshold projection went from β = 1 to β = 128 following the update law $\beta_{i+1} = 2\beta_i$.

The optimization was made restricting the design variable to 1 in an enclosing of thickness t around the design domain. This restriction was applied to guarantee that the actuator remains closed during the optimization process. The optimization was carried out with different values for the bulk modulus of the fluid region to verify its influence in the results. Figure 4 and Tab. 1 present results for air, water, and a highly incompressible fluid.

(a) Design for K_f = 101 kPa (air) (b) Design for K_f = 2.15 GPa (water) (c) Design for $K_f = 10^6 K_s$

Figure 4: Results for bending actuator optimization.

Table 1: Bending actuator optimization output.

Example	K_f	Figure	Objective Function	Discreteness
Air	101 kPa	4a	50.9 mm	2.3%
Water	2.15 GPa	4b	25.7 mm	2.5%
Highly incompressible	$10^6 K_s$	4c	18.3 mm	2.8%

The topology obtained for air bulk modulus differs from the ones obtained for water and highly incompressible fluid. As it does not have significant changes to the actuator walls, there is some indication of a wrong design. To test the designs we run the forward model of each optimized design for each material model. Analyzing the objective function values of Tab. 2 it is clear that the air design is not optimized because it gives negative values of objective function for water and highly incompressible fluid.

The problem of the optimization using air bulk modulus is that the displacements at fluid region were large, violating the small displacements assumption made during modelling. This makes the problem ill posed and the convergence is not guaranteed. So, it is necessary to keep the input load and the bulk modulus compatible to avoid large displacements.

Table 2: Cross simulation of optimized topologies for bending actuator.

Example	K_f	Figure 4a	Figure 4b	Figure 4c
Air	101 kPa	50.9 mm	28.1 mm	21.3 mm
Water	2.15 GPa	-2.9 mm	25.7 mm	20.0 mm
Highly incompressible	$10^6 K_s$	-1.3 mm	22.4 mm	18.3 mm

We also experimented a continuation technique at SIMP parameter going from a penalization factor of 1 to 5 with a increase of a unit at each step. In this case, we did not find a bad design for air material properties (Fig. 5a). Also, the topologies for water and highly incompressible fluid presented better objective function values (Tab. 3). These results encourage the use of continuation techniques with this formulation.

Table 3: Bending actuator output for optimization with SIMP continuation.

Example	K_f	Figure	Objective Function	Discreteness
Air	101 kPa	5a	34.7 mm	1.9%
Water	2.15 GPa	5b	33.9 mm	1.3%
Highly incompressible	$10^6 K_s$	5c	37.0 mm	2.2%

(a) Design for K_f = 101 kPa (air) (b) Design for K_f = 2.15 GPa (water) (c) Design for $K_f = 10^6 K_s$

Figure 5: Results for bending actuator optimization with SIMP continuation.

We also present the displacements of designs from Fig. 5 in Fig. 6. It is possible to see how the enlargement of the parts of the wall decrease its displacement favoring the movement in the desired direction. The displacements are magnified 5 times for better visualization of results.

(a) Displacement for K_f = 101 kPa (b) Displacement for K_f = 2.15 GPa (c) Displacement for $K_f = 10^6 K_s$

Figure 6: Displacement for bending actuator optimization with SIMP continuation.

We did some experiments with different threshold values, but the convergence for $\eta = 0.5$ was better. For $\eta = 1$ (minimum length scale on void/fluid phase), the enclosing region that is restricted to be 1 at design field opens at physical domain making the model invalid. For $\eta = 0$ (minimum length scale on solid phase), the enclosing region becomes thicker and the result does not represent an optimized topology.

Linear soft actuator

To evaluate the formulation for other design problems, we also optimized the design problem presented in Fig. 7. The difference from this problem to the one presented in Fig. 3 is the position of the output port that is now centered at right wall.

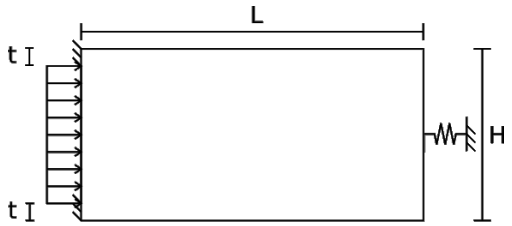

Figure 7: Design domain for the linear soft actuator.

To keep more balance between the contribution of the walls of the actuator, we optimized a square design domain of sides L = H = 10 m. With the exception of the dimensions, we considered the same parameters of the bending actuator example and followed the continuation of SIMP parameter because it yields better designs. The results are presented in Fig. 8 and Tab. 4. The displacement fields are presented in Fig. 9.

Again, the results for water and highly incompressible fluid are similar. They maximized the output displacement changing the thickness of the walls. The deformation of the upper and lower walls of the actuator due to internal pressure reduce the objective function. On the other hand. the deformation of the right wall increase the objective function. So, optimized topologies have stiffer (thicker) lower and upper walls and compliant (thinner) right wall.

The topology obtained in the optimization using air parameters presents no topological features that would maximize

the output displacement because all walls have similar thickness. This indicates that the convergence for air bulk modulus was worse than for the other fluids.

(a) Design for K_f = 101 kPa (air) (b) Design for K_f = 2.15 GPa (water) (c) Design for $K_f = 10^6 K_s$

Figure 8: Results for linear actuator optimization.

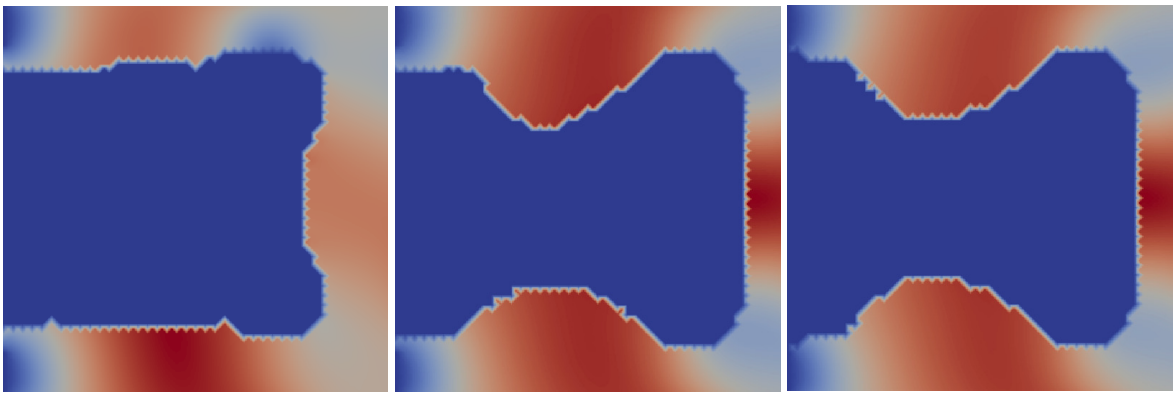

(a) Design for K_f = 101 kPa (air) (b) Design for K_f = 2.15 GPa (water) (c) Design for $K_f = 10^6 K_s$

Figure 9: Displacements for linear actuator optimization.

Table 4: Linear actuator optimization output displacement.

Example	K_f	Figure	Objective Function	Discreteness
Air	101 kPa	8a	0.26 mm	2.4%
Water	2.15 GPa	8b	0.42 mm	2.0%
Highly incompressible	$10^6 K_s$	8c	0.40 mm	1.8%

To evaluate objectively the differences between the obtained topologies we simulated each topology with each material model and the results are presented in Tab. 5. According to the table the topology obtained for air bulk modulus really presents worse performance even for simulations using air material model. This indicates that the convergence for lower bulk modulus values is again worse than for higher values and it is in accordance with our intuitive analysis because the model has no topological features at walls that would maximize the output displacement.

CONCLUSIONS

The proposed methodology was able to design pneumatic and hydraulic actuators by the topology optimization method. The convergence for compressible materials (low bulk modulus) is less stable because the problem can become

Table 5: Cross simulation of optimized topologies for linear actuator.

Example	K_f	Figure 8a	Figure 8b	Figure 8c
Air	101 kPa	0.26 mm	0.39 mm	0.38 mm
Water	2.15 GPa	0.14 mm	0.42 mm	0.43 mm
Highly incompressible	$10^6 K_s$	0.13 mm	0.40 mm	0.40 mm

ill posed due to large displacements in fluid domain. Continuation techniques can be employed to help in the stabilization of the problem even with the violation of small displacement assumption in the fluid domain, but it is better to model the problem using incompressible materials because it would yield results that are close to the ones obtained in a stable optimization of compressible materials and there are no risks of wrong results due to ill-posedness.

The difference in stiffness along the actuators wall is the mechanism that provides the movement. Therefore, the topologies features were concentrated at actuators walls as expected. Features in the interior of the domain have low impact on the walls stiffness and they did not appear in optimized results.

The design variables had to be restricted at the walls of the domain because the model can not model pressure gradients in the fluid domain. This limited the optimization of exterior surfaces of the actuators.

The next steps to continue this work on topology optimization of soft actuators is to consider 3D domains for equivalent design problems and to fabricate the obtained topologies to verify the accordance of physical experiments and numerical simulations. Future works would involve the consideration of finite deformations and nonlinear material models that represent better to behavior of elastomeric materials.

REFERENCES

Allaire, G., Jouve, F., Toader, A.M., 2002, "A level-set method for shape optimization", Comptes Rendus Mathematique, Vol. 334(12), pp. 1125-1130.

Alnaes, M.S., Blechta, J., Hake, J., Johansson, A., Kehlet, B., Logg, A., Richardson, C., Ring, J., Rognes, M.E., Wells, G.N., 2015, "The FEniCS Project Version 1.5", Archive of Numerical Software, Vol. 3, 2015.

Bendsøe, M.P., Kikuchi, N., 1988, "Generating optimal topologies in structural design using a homogenization method", Computer Methods in Applied Mechanics and Engineering, Vol. 71(2), pp. 197-224.

Bendsøe, M.P., 1989, "Optimal shape design as a material distribution problem", Structural Optimization, Vol. 1(4), pp. 193-202.

Borrvall, T., Petersson, J., 2002, "Topology optimization of fluids in Stokes flow", International Journal for Numerical Methods in Fluids, Vol. 41, pp. 77-107.

Bourdin, B., Chambolle, A., 2003, "Design-dependent loads in topology optimization", ESAIM: Control, Optimisation and Calculus of Variations, Vol. 9, pp. 19-48.

Farrell, P.E., Ham, D.A., Funke, S.W., Rognes, M.E., 2013, "Automated Derivation of the Adjoint of High-Level Transient Finite Element Programs", SIAM Journal on Scientific Computing, Vol. 35(4), pp. 369-393.

Funke, S.W., Farrell, P.E., 2013, "A framework for automated PDE-constrained optimisation", "arXiv:1302.3894".

Galloway, K.C., Polygerinos, P., Walsh, C.J. and Wood R.J., 2013, "Mechanically programmable bend radius for fiber-reinforced soft actuators", 16th International Conference on Advanced Robotics (ICAR).

Gersborg-Hansen, A., Bendsøe, M.P., Sigmund, O., 2006, "Topology optimization of heat conduction problems using the finite volume method", Structural and Multidisciplinary Optimization, Vol. 31(4), pp. 251-259.

Guest, J.K., Prévost, J.H., Belytschko, T., 2004, "Achieving minimum length scale in topology optimization using nodal design variables and projection functions", International Journal for Numerical Methods in Engineering, Vol. 61(2), pp. 238-254.

Hiller J. and Lipson H., 2012, "Automatic Design and Manufacture of Soft Robots", IEEE Transactions on Robotics, Vol. 28, pp. 457-466.

Lazarov, B.S. and Sigmund, O., 2010, "Filters in topology optimization based on Helmholtz-type differential equations", International Journal for Numerical Methods in Engineering, Vol. 86, pp. 765-781.

Logg, A., Mardal, -A., Wells, G.N. et al, 2012, Automated Solution of Differential Equations by the Finite Element Method, Springer, 2012.

Mosadegh, B. et al, 2014, ”Pneumatic Networks for Soft Robotics that Actuate Rapidly”, Advanced Functional Materials, Vol. 24, pp. 2163-2170.

París, J., Navarrina, F., Colominas, I., Casteleiro, M., 2008, ”Topology optimization of continuum structures with local and global stress constraints”, Structural and Multidisciplinary Optimization, Vol. 39(4), pp. 419-437.

Pedersen, C.B.W., Buhl, T. and Sigmund, O., 2001, ”Topology synthesis of large-displacement compliant mechanisms”, International Journal for Numerical Methods in Engineering, Vol. 50, pp. 2683-2705.

Sigmund, O. and Clausen, P.M., 2007, ”Topology optimization using a mixed formulation: An alternative way to solving pressure load problems”, Computer Methods in Applied Mechanics and Engineering, Vol. 196, pp. 1874-1889.

Sokolowski, J., Zochowski, A., 1999, ”On the Topological Derivative in Shape Optimization”, SIAM Journal on Control and Optimization, Vol. 37(4), pp. 1251-1272.

Suzumori, K., 1996, ”Elastic materials producing compliant robots”, Robotics and Autonomous Systems, Vol. 18, pp. 135-140.

Wang, F., Lazarov B. S., Sigmund O., 2010, ”On projection methods, convergence and robust formulations in topology optimization”, Structural and Multidisciplinary Optimization, Vol. 43, pp. 767-784.

Wächter, A. and Biegler, L.T., 2006, ”On the Implementation of a Primal-Dual Interior Point Filter Line Search Algorithm for Large-Scale Nonlinear Programming”, Mathematical Programming, Vol. 106(1), pp. 25-57.

RESPONSIBILITY NOTICE

The author(s) is (are) the only responsible for the printed material included in this paper.